Vol.02 No.02 (2026) 32-51

Sustainable in Energy Science and Technology

https://ojs.polmed.ac.id/index.php/SiEST

Sustainable Design of a Compact 3+1 DOF Desktop Robotic Arm for Energy-Efficient Automation

Muhammad Shobri[1], Ignatius Budi Sutanto Hadisujoto[1*], Djati Wibowo[1]

Department of Mechanical Engineering, Faculty of Engineering and Technology, Sampoerna University, Jakarta, 12780, Indonesia

*Corresponding Author: ignatius.hadisujoto@sampoernauniversity.ac.id

Graphical Abstract

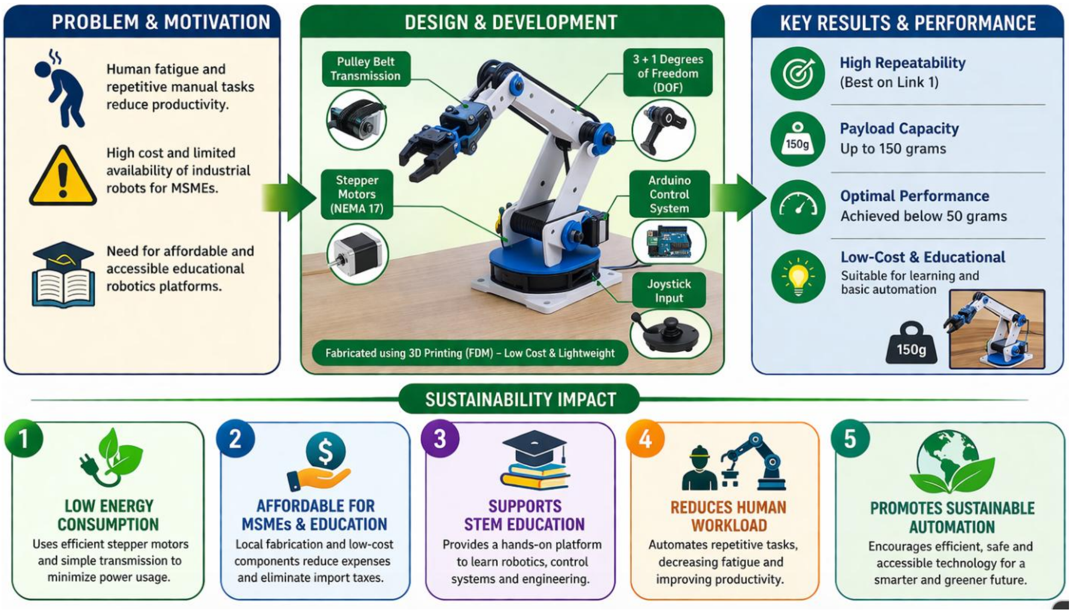

Highlights

- Low-cost 3+1 DOF robotic arm developed for sustainable automation.
- Energy-efficient stepper motor with pulley system improves torque.
- Achieves high repeatability with optimal performance below 50 g load.
- Arduino-based control enables accessible robotics learning platform.
- Supports MSMEs and education through affordable automation solutions.

ARTICLE INFO

Keywords:
Robotic Arm; Stepper Motor; Pulley Belt Transmission; Repetitive Task Automation; Educational Robotics; Accuracy and Precision

Article history:
Received June 04, 2026
Revised July 29, 2026
Accepted August 17, 2026
Available online August 17, 2026

ABSTRACT

Fatigue, human error, and reduced productivity are common challenges in industrial operations involving repetitive manual tasks. In response, this paper presents the design, fabrication, and performance evaluation of an affordable, low-cost desktop robotic arm featuring 3+1 degrees of freedom (DoF) integrated with a servo-driven gripper. The mechanical structure was modeled in SolidWorks and fabricated via Fused Deposition Modeling (FDM) 3D printing utilizing Polylactic Acid (PLA) material. To optimize torque transmission and ensure smooth, low-backlash operation, actuation is achieved via NEMA stepper motors coupled with a pulley belt transmission system, controlled by an Arduino microcontroller. Test experiments were conducted to assess mechanical reliability, specifically focusing

https://doi.org/10.51510/siest.v2i2.3371

on positioning repeatability using an analog dial indicator and payload capacity constraints. Experimental results indicate that while the primary link maintains excellent positional consistency across successive cycles, mechanical joint play and inconsistent belt tension introduce slight positional deviations along the base and secondary link axes. Furthermore, load testing demonstrated a maximum payload capacity of 150 grams, with optimal operational stability achieved under 50 grams before structural strain occurs. The developed prototype demonstrates a cost-effective automation architecture for light industrial tasks and offers a robust, accessible open-source platform for robotics education. Ongoing development focuses on integrating feedback sensors, such as encoders and limit switches, to transition the platform from manual control to full closed-loop automation.

1. Introduction

The rapid advancement of industrial automation has positioned robotic arms as essential components in modern manufacturing due to their ability to enhance productivity, precision, and operational flexibility. Robotic arms are widely implemented to perform repetitive, labor-intensive, and high-risk tasks with high repeatability and minimal variation, thereby improving production efficiency and product quality [1–3]. Beyond improving production efficiency, robotic automation significantly enhances occupational safety by minimizing human exposure to hazardous, repetitive, and ergonomically challenging environments [4]. However, widespread adoption remains low among micro, small, and medium-sized enterprises (MSMEs) in developing countries due to high capital costs, reliance on imported technologies, and a lack of accessible technical expertise [5–7]. Consequently, many small-scale industries continue to rely on manual labor, which induces physical fatigue, decreases concentration, and introduces operational inconsistencies that compromise quality and workplace safety.

From a sustainability perspective, the need for affordable and energy-efficient automation systems has become increasingly important. Sustainable engineering emphasizes not only environmental considerations but also economic feasibility and social impact, particularly in resource-constrained environments. In this context, the development of low-cost robotic systems can contribute to sustainable industrial practices by improving resource efficiency, reducing human workload, and enabling consistent production processes [8]. Furthermore, automation systems that utilize energy-efficient components and lightweight materials can significantly reduce energy consumption compared to conventional heavy industrial robots. The integration of sustainable design principles—such as material efficiency, modularity, and recyclability—into robotic systems further enhances their environmental performance and lifecycle sustainability [9].

The demand for automation is also driven by the limitations of human labor in repetitive operations. Continuous manual tasks often lead to physical fatigue, decreased concentration, and inconsistent performance, which negatively impact production quality and operational reliability [10]. Robotic arms provide a viable solution by offering high precision, repeatability, and continuous operation without performance degradation. However, conventional industrial robots are often designed for high-load and high-precision applications, resulting in complex systems with high energy consumption and maintenance requirements [11]. Therefore, there is a growing interest in developing simplified robotic systems that can perform basic tasks efficiently while maintaining low energy consumption and cost. Such systems are particularly relevant for small-scale industries and educational institutions that require affordable and accessible automation technologies.

In the field of engineering education, robotic arms play a crucial role as practical learning tools that facilitate the understanding of robotics, control systems, kinematics, and mechanical design. The integration of robotics into educational curricula promotes hands-on learning and enhances students' technical competencies, creativity, and problem-solving skills [12]. However, many educational institutions face challenges in acquiring commercial robotic systems due to high procurement costs and limited budgets. Consequently, the development of low-cost robotic platforms using open-source hardware, such as Arduino, and locally available materials has gained significant attention. These platforms not only reduce costs but also provide flexibility for customization and experimentation, thereby supporting sustainable education and technological development [13].

Recent studies demonstrate that robotic arms with limited degrees of freedom (DoF), particularly 3-DoF configurations, provide an ideal balance of functionality and cost-effectiveness for basic industrial tasks like pick-and-place operations [14–16]. While various robotic configurations—such as articulated, SCARA, cylindrical, and collaborative robots (cobots)—excel in specific complex or shared workspaces [18–21], small-scale applications benefit most from simplified mechanical and control designs. A critical factor driving both cost and efficiency is the transmission system. While planetary gears, cycloidal drives, and harmonic drives offer high torque and precision, they introduce prohibitive costs and mechanical complexity [23–25]. Conversely, pulley belt systems offer a lightweight, mechanically simple, and highly efficient alternative for power transmission. When paired with actuators, stepper motors present a more cost-effective and simpler integration choice for open-source platforms than complex closed-loop servo motors or high-speed DC motors that lack inherent positioning accuracy [26–28].

To address the need for accessible, sustainable automation, this study focuses on the design and development of a small desktop robotic arm with 3+1 degrees of freedom (DoF). The system integrates stepper motors with a pulley belt transmission system to achieve enhanced torque performance and precise motion control while minimizing production costs.

2. Methodology

2.1 Methodology Flow

The development framework for the 3+1 DoF desktop robotic arm was meticulously structured into a sequential, multi-phase engineering pipeline. As illustrated in the system workflow in Figure 1, the methodology transitions systematically from theoretical constraint definition to computer-aided design (CAD), kinetic force verification, additive manufacturing prototyping, hardware integration, and experimental validation. The detailed design requirements are presented in Table 1, highlighting the integration of sustainable engineering criteria into the robotic system.

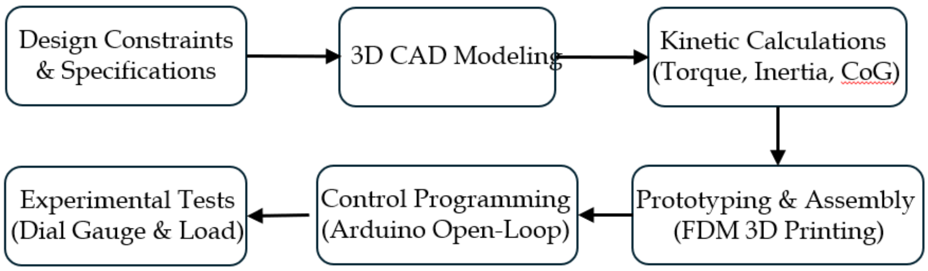

Figure 1. Methodology Flow

Table 1. Specification of the Robot Needed

Specification	
Primary	Small desktop size (approx. 20 x 20 cm)
	Can carry load weight of 50 - 100 gr
	Easy to use/control
	Weight less than 5 kg
	Maximum reach 20 cm (or more) from the base
Secondary	Able to be operated for a long time
	Quite when being operated
	Have a smooth movement
Tertiary	Aesthetic looks
	Low cost to produce
	Spare part components easy to find

2.2 Design and Simulation

The robotic arm was designed using SolidWorks, where conceptual ideas were translated into detailed 3D CAD models. Each component was modeled and assembled virtually to evaluate motion range, mechanical interference, and energy-efficient movement prior to fabrication. A pulley belt transmission system was selected due to its ability to reduce friction losses, operate with lower noise, and improve torque efficiency compared to conventional gear systems. Stepper motors were employed for actuation due to their precise control, low power requirements, and suitability for energy-efficient automation systems [4]. The simulation stage enabled optimization of structural design and motion paths, ensuring minimal energy wastage, proper alignment, and mechanical reliability before proceeding to fabrication.

2.3 Mechanical Analysis

Mechanical analysis was conducted to ensure that the robotic arm operates efficiently under both static and dynamic conditions while minimizing energy demand. The key parameters of the robotic links, including mass, length, and distance from the rotational axis, are summarized in Table 2. The center of gravity (CoG) of the assembled robotic system was determined using SolidWorks mass property analysis to enhance stability and reduce unnecessary energy consumption during operation. Proper CoG positioning minimizes torque requirements and improves system efficiency. This simulation-based approach has been validated in previous studies for accurate prediction of mass distribution and mechanical performance [29, 30]. Static torque was calculated by evaluating gravitational forces acting on each component relative to the rotational axis, while dynamic torque was estimated based on the moment of inertia and angular acceleration.

Table 2. Parameters of the Robot's links

Parts Name	Mass (Kg)	Weight (N)
Crank	5×10^{-3}	49.05×10^{-3}
Coupler	8×10^{-3}	78.48×10^{-3}
Follower	26×10^{-3}	255.06×10^{-3}
Base Link	51×10^{-3}	500.31×10^{-3}
Stabilizer 1	30×10^{-3}	294.3×10^{-3}
Stabilizer 2	13×10^{-3}	127.53×10^{-3}
Stabilizer 3	42×10^{-3}	412.02×10^{-3}
Full Mount Gripper	76×10^{-3}	745.56×10^{-3}

2.4 Prototyping and Assembly

Following design validation, the robotic arm components were fabricated using fused deposition modeling (FDM) with an Anycubic Kobra 2 Pro 3D printer. Additive manufacturing was selected as it minimizes material waste and supports sustainable production practices. Polylactic acid (PLA) filament was used and 15 % infill density was applied to minimize material usage while maintaining structural integrity. All components were assembled systematically, integrating mechanical and electronic subsystems, including links, pulleys, bearings, stepper motors, and Arduino microcontroller.

2.5 Programming and Experimental Evaluation

The robotic arm was programmed using Arduino IDE to enable manual control using joysticks. Performance evaluation was conducted using two primary experiments: the dial indicator test and the load test. The dial indicator setup, shown in Figure 2 was used to measure displacement deviations and assess repeatability, which is critical for reducing energy losses due to positioning errors. The load tests were evaluated at the maximum payload capacity by incrementally increasing the applied weight. This test provided insights into energy efficiency, torque utilization, and structural robustness of the system under varying load conditions. The experimental results demonstrated the feasibility of developing a low-cost, energy-efficient robotic arm using sustainable materials and design principles, making it suitable for educational and small-scale automation applications.

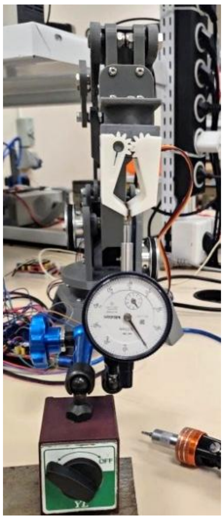

Figure 1. Mounting Dial Indicator to the Robot

The load test was conducted by initially attaching a mass weighing 10 grams securely to the gripper and actuating the crank link to lift the load while observing the system's movement. Another 10 grams of mass was incrementally added to increase the load. In cases where lifting became difficult, the base link and robot base were activated to assist the motion. The load was progressively increased until the robotic arm was no longer able to lift. Finally, the maximum load capacity of the robotic arm was recorded, concluding the test.

3. Results and Discussion

3. 1 CAD Design and Component Development

The three-dimensional (3D) design of the robotic arm components was developed using SolidWorks, enabling detailed visualization, interference checking, and structural verification prior to fabrication. The assembly of the robotic arm is shown in Figures 3 and 4, and the protype is shown in Figure 5.

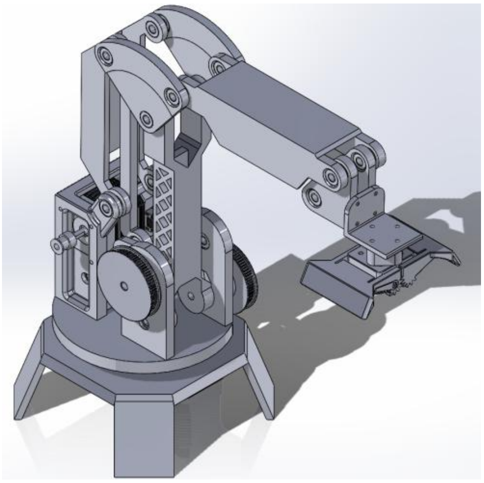

Figure 2. Full Assembly of the Robot Arm in Isometric View

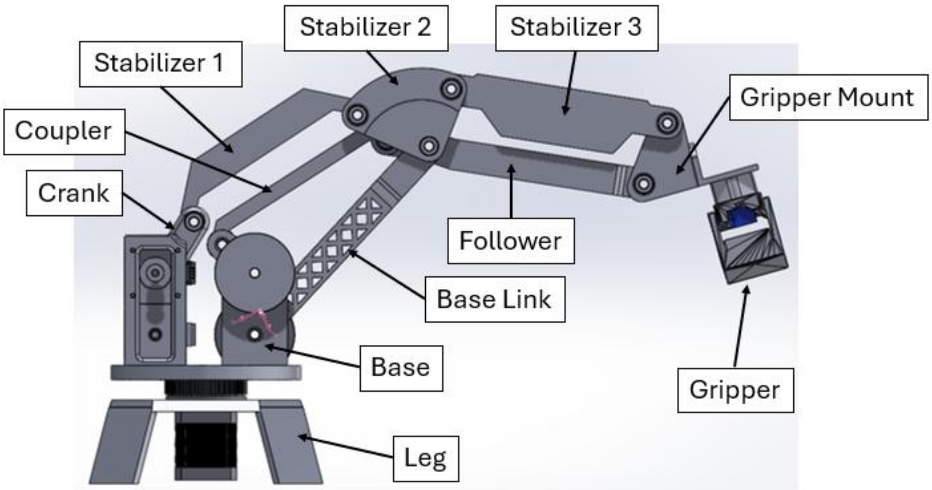

Figure 3. Full Assembly of the Robot Arm in Side View

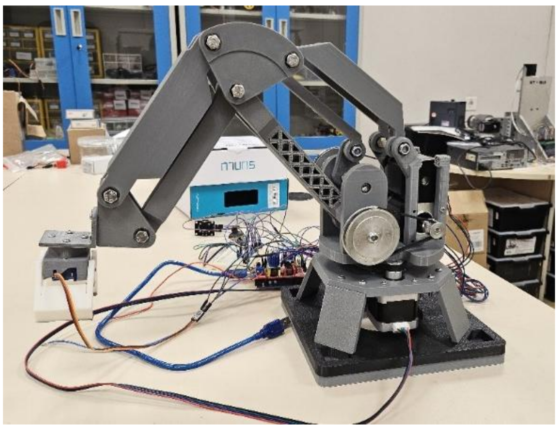

Figure 4. Robot arm prototype

3. 2 Torque Analyses

The center of gravity (CoG) of the robotic arm is shown in Figure 6, utilizing SolidWorks mass properties feature. The CoG location within the base region minimizes the risk of tipping and enhances overall system stability.

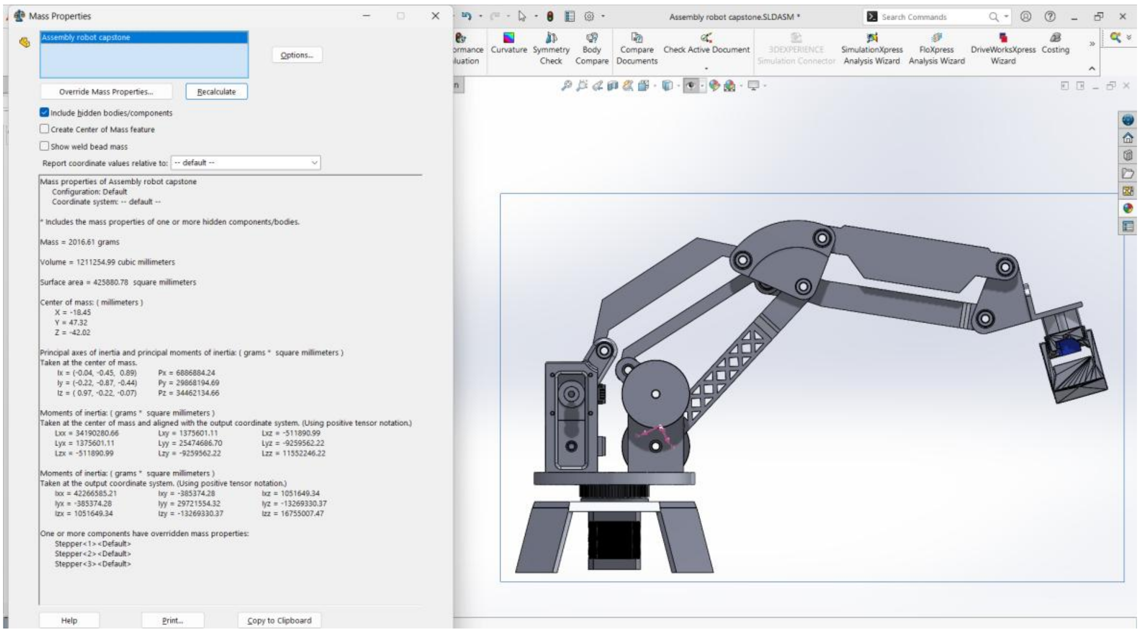

Figure 5. Center of Gravity of the system by SolidWorks (Purple Mark)

The parameters for calculating the static torque of the robotic arm are illustrated in Figure 7 and listed in Table 3.

Two NEMA 17 SL42TH48-1684A stepper motors were used to rotate the base link and the crank. A NEMA 17 has rated torque 0.55 Nm. Pair of timing pulleys are used to increase the stepper motor torque. The pairing is 20 teeth and 80 teeth pulleys using 2 GT specification. Taking account of the diameter dimensions (d) of the pulleys, the increased torque (T) is:

$$\frac{d_1}{d_2} = \frac{T_1}{T_2}$$

$$T_2 = \frac{55.5}{9.5} \times 0.55 = 3.21 \text{ Nm}$$

The maximum static torque to hold the arm can be calculated when the arm extends the longest. Based on Figures 7, the weights in Table 2, and the lengths in Table 3, the free body diagram can be established, and the static torque (T) can be derived from the following equation.

$$\sum M_{static} = T - W_{crank}(L_1) - W_{coupler}(L_2) - W_{folower}(L_3) - W_{gripper}(L_4)$$
$$-W_{BaseLink}(L_5) - W_{stablizer1}(L_6) - W_{stablizer2}(L_7)$$
$$-W_{stablizer3}(L_8) = 0$$

Inserting the properties of weights and related lengths, the maximum static torque T is 0.408 Nm.

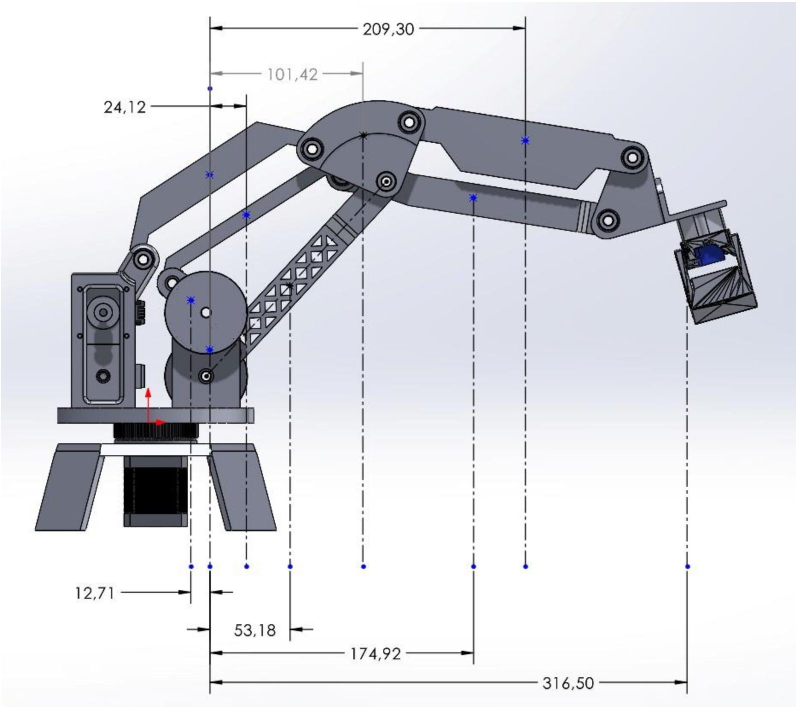

Figure 6. Horizontal Dimension of Links' COG to Assembly's COG (SolidWorks)

Table 3. Horizontal Dimension of Links' COG to Assembly's COG (Data Table)

Parts Name	Distance From CG to Assembly CG (m)
Crank	12.71×10^{-3}
Coupler	24.12×10^{-3}
Follower	174.92×10^{-3}
Base Link	53.18×10^{-3}
Stabilizer 1	0
Stabilizer 2	101.45×10^{-3}
Stabilizer 3	209.30×10^{-3}
Full Mount Gripper	316.50×10^{-3}

To determine the dynamics torque, angular velocity and acceleration are obtained from the setting parameters controlling the robot arm movement. The stepper motor is set to 200 step/rev or 1.8^o/step. The stepper motor maximum speed is set 100 steps/sec and 800 step/sec^2 for the acceleration. These convert to angular velocity of 5 rev/sec or 31.24 rad/sec. From these, the acceleration is 25.14 rad/sec^2.

To compute the moment of inertia (I) for each link of the robotic arm, each link is simplified as a rectangular shape to its irregular form. The formula utilized is given below.

$$I = \frac{1}{12}(m)(L^2) + (m)(d^2)$$

Where m is the mass of the link, L is the length of the link, and d is the distance from the robot CoG to the link's CoG.

To simplify, all the result and know parameters are shown in Table 4 and Figure 8 below.

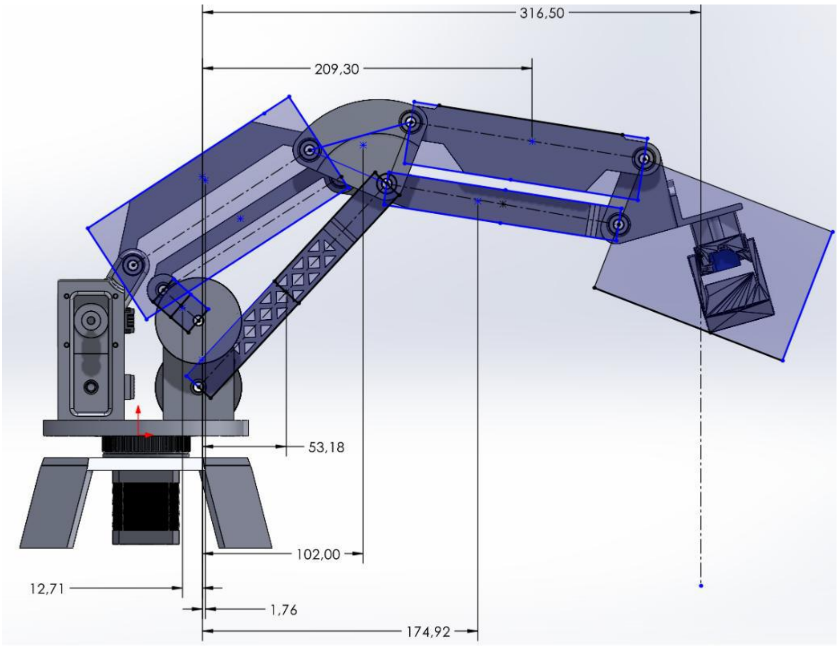

Figure 8. Dimension Parameters of the Robot Arm.

Table 4. Calculation Result of the Moment Inertia of the links

Parts	Mass (kg)	Length (m)	Distance d (m)	Inertia I (kg.m²)
Crank	0.005	0.0295	0.01271	5.69×10^{-6}
Coupler+Stabilizer1	0.038	0.153	0.00176	7.33×10^{-4}
Follower	0.026	0.1495	0.17492	8.24×10^{-3}
Base Link	0.051	0.176	0.05318	2.37×10^{-3}
Stabilizer 3	0.042	0.150	0.2093	2.02×10^{-2}
Mount & Gripper	0.076	0.1285	0.3165	7.65×10^{-2}

From Table 4, it can be calculated that total inertia is 0.105 kg. Finally, the maximum dynamic torque is the total inertia multiplied by the angular acceleration of 25.14 rad/sec², which results 2.64 Nm of torque.

3. 3 Dial Indicator Test-Base Movement

The dial indicator test results for the base axis (Tables 5–7 and Figure 8) reveal significant variability and low repeatability. Trial 1 showed deviations ranging from 0.18 mm to 0.62 mm, while Trials 2 and 3 exhibited severe inconsistencies, with most cycles failing to return to the reference position. These findings indicate poor positional accuracy and instability in the base movement. The observed inaccuracies are primarily attributed to insufficient tension in the pulley belt, which resulted in slippage between the motor and the rotating base. Belt slippage is a well-documented issue in transmission systems and can lead to cumulative positioning errors over repeated cycles [44]. The results emphasize the importance of proper tensioning and mechanical coupling in ensuring reliable robotic performance. Improving the transmission system, either through optimized belt tension or alternative drive mechanisms, is expected to significantly enhance accuracy and repeatability.

Table 4. Robot Base Movement Trial 1 Dial Indicator Test

Cycle	Reading (mm) Original Position	Final Position
1	0.60 mm	0.22 mm
2		0.23 mm
3		0.19 mm
4		0.18 mm
5		0.29 mm
6		0.34 mm
7		0.31 mm
8		0.62 mm
9		0.49 mm
10		0.44 mm

Table 5. Robot Base Movement Trial 2 Dial Indicator Test

Cycle	Reading (mm) Original Position	Final Position
1	0 mm (Touch the dial)	Did Not Touch Dial
2		Did Not Touch Dial
3		Did Not Touch Dial
4		Did Not Touch Dial
5		Did Not Touch Dial
6		Did Not Touch Dial
7		Did Not Touch Dial
8		Did Not Touch Dial
9		Did Not Touch Dial
10		Did Not Touch Dial

Table 6. Robot Base Movement Trial 3 Dial Indicator Test

Cycle	Reading (mm) Original Position	Final Position
1	0 mm (Touch the dial)	Did Not Touch Dial
2		Did Not Touch Dial
3		0.92 mm
4		0.90 mm
5		0.35 mm
6		Did Not Touch Dial
7		Did Not Touch Dial

Cycle	Reading (mm) Original Position	Final Position
8		Did Not Touch Dial
9		Did Not Touch Dial
10		Did Not Touch Dial

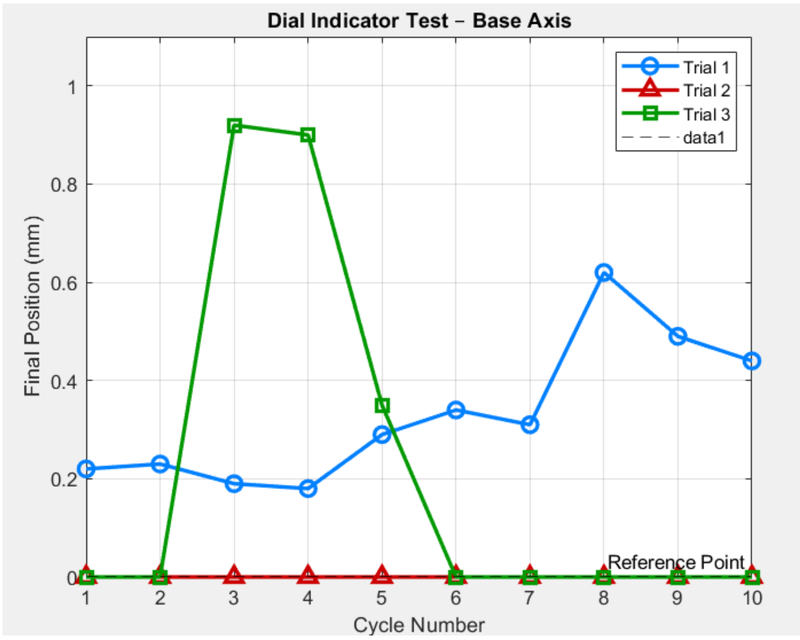

Figure 7. Dial Indicator Test Plot of Base Movement

3. 4 Dial Indicator Test-Link Two Movement

The link two axis results (Tables 8–10 and Figure 9) demonstrate high repeatability but limited accuracy. The system consistently returned to similar positions within each trial; however, a systematic offset from the reference position was observed. Trial 1 exhibited deviations between 0.30 mm and 0.37 mm, Trial 2 between 0.08 mm and 0.11 mm, and Trial 3 showed overshoot behavior between 1.04 mm and 1.09 mm. This consistent offset indicates the presence of systematic mechanical error rather than random variation. Inspection revealed that the pulley belt tension was adequate; however, a damaged spacer in the crank mechanism caused misalignment. Structural misalignment is known to introduce consistent positional errors in robotic linkages, affecting accuracy while maintaining repeatability [45]. These findings highlight that structural integrity is as critical as actuation performance in achieving accurate motion. Replacing the damaged component and improving assembly precision are necessary to eliminate this systematic error.

Table 7: Robot Link Two Movement Trial 1 Dial Indicator Test

Cycle	Reading (mm) Original Position	Final Position
1	1 mm	0.37 mm
2		0.35 mm

Cycle	Reading (mm) Original Position	Final Position
3		0.34 mm
4		0.33 mm
5		0.32 mm
6		0.31 mm
7		0.31 mm
8		0.30 mm
9		0.31 mm
10		0.32 mm

Table 8: Robot Link Two Movement Trial 2 Dial Indicator Test

Cycle	Reading (mm) Original Position	Final Position
1	1 mm	0.09 mm
2		0.10 mm
3		0.10 mm
4		0.11 mm
5		0.11 mm
6		0.10 mm
7		0.10 mm
8		0.09 mm
9		0.09 mm
10		0.08 mm

Table 9: Robot Link Two Movement Trial 3 Dial Indicator Test

Cycle	Reading (mm) Original Position	Final Position
1	1 mm	1.09 mm
2		1.04 mm
3		1.05 mm
4		1.04 mm
5		1.05 mm
6		1.05 mm
7		1.05 mm
8		1.06 mm
9		1.06 mm
10		1.06 mm

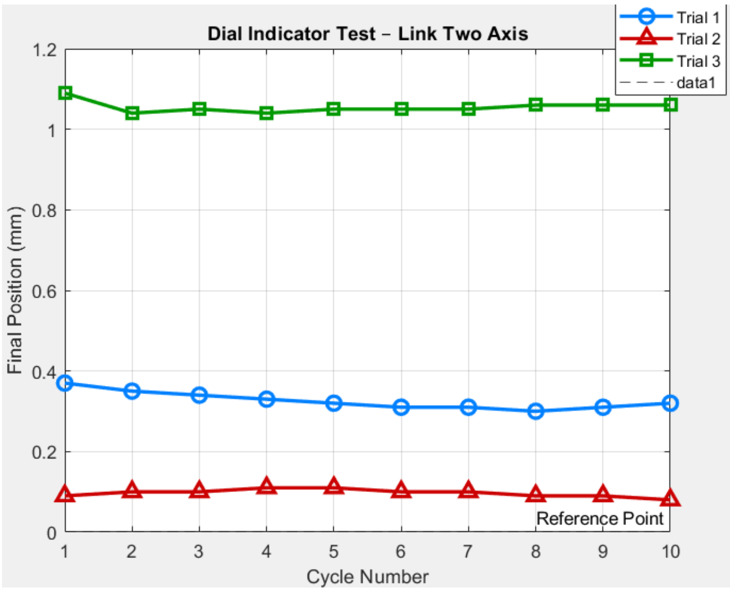

Figure 8: Dial Indicator Test Plot of Link Two Movement

3. 5 Dial Indicator Test-Link One Movement

The link one axis (Tables 11–13 and Figure 10) demonstrated the highest performance among all tested components. Trials 1 and 2 showed extremely consistent results, with deviations of only 0.02–0.03 mm, indicating excellent precision and repeatability. Trial 3 exhibited temporary variation, likely due to thermal effects or minor dynamic disturbances. The superior performance of link one is attributed to optimal belt tension, rigid structural connections, and minimal mechanical backlash. These factors are essential for achieving high positioning accuracy in robotic systems [46]. The slight deviation observed in Trial 3 is consistent with known effects of thermal buildup in motor drivers, which can influence system performance during prolonged operation [47]. The results confirm that stable mechanical configuration and proper alignment are critical for precision control.

Table 10. Robot Link One Movement Trial 1 Dial Indicator Test

	Reading (mm)	
Cycle	Original Position	Final Position
1	1 mm	0.03 mm
2		0.03 mm
3		0.03 mm
4		0.03 mm
5		0.03 mm
6		0.03 mm
7		0.03 mm
8		0.03 mm
9		0.03 mm
10		0.03 mm

Table 11. Robot Link One Movement Trial 2 Dial Indicator Test

Cycle	Reading (mm) Original Position	Final Position
1	1 mm	0.03 mm
2		0.03 mm
3		0.03 mm
4		0.03 mm
5		0.03 mm
6		0.03 mm
7		0.03 mm
8		0.02 mm
9		0.02 mm
10		0.02 mm

Table 12. Robot Link One Movement Trial 3 Dial Indicator Test

Cycle	Reading (mm) Original Position	Final Position
1	1 mm	0.63 mm
2		0.63 mm
3		0.59 mm
4		0.51 mm
5		0.48 mm
6		0.45 mm
7		0.39 mm
8		0.25 mm
9		0.29 mm
10		0.48 mm

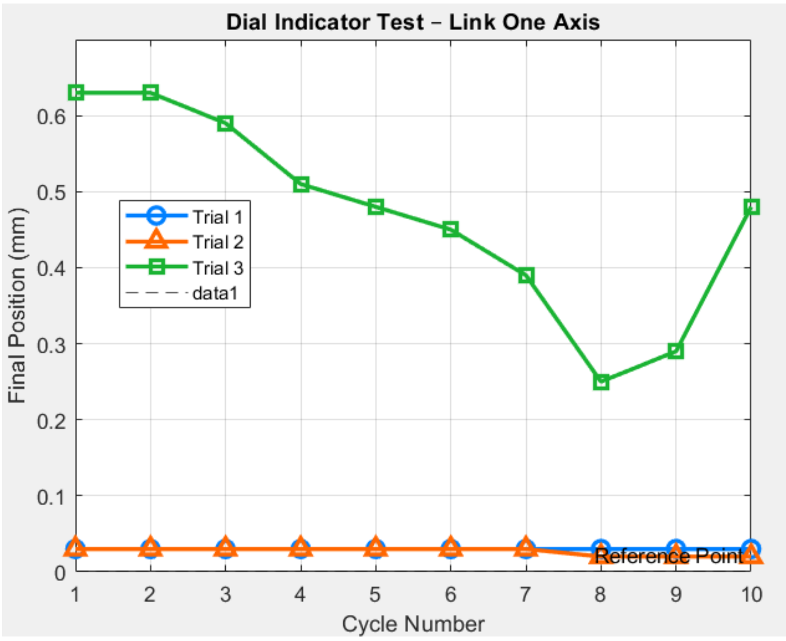

Figure 9. Dial Indicator Test Plot of Link One Movement

3. 6 Load Test Performance

The load test results (Table 14 and Figure 11) demonstrate the relationship between payload and system performance. The robotic arm operated efficiently for loads up to 50 g, with no observable performance degradation. Beyond this threshold, the system exhibited increasing difficulty in lifting, with maximum capacity reached at 150 g. The decrease in performance with increasing load is attributed to the limited torque output of the stepper motor and the mechanical constraints of the linkage system. As load increases, the torque required to overcome gravitational forces also increases, eventually exceeding the motor's capability [48]. This behavior is consistent with established robotic load–torque relationships. The results highlight the trade-off between lightweight design and load capacity. While the use of lightweight materials such as PLA contributes to energy efficiency and sustainability, it limits structural strength and payload capability. Future improvements may involve optimizing gear ratios or using higher torque motors, although such modifications may increase energy consumption [49]. The findings confirm that the robotic arm is well-suited for light-duty applications, particularly in educational and low-load industrial scenarios.

Table 13. Load Test Result

Load Test Weight (g)	Hoisted (Yes / No)	Performance (%)
± 10 g	Yes	100%
± 20 g	Yes	100%
± 30 g	Yes	100%
± 40 g	Yes	100%
± 50 g	Yes	100%
± 60 g	Yes	95%
± 70 g	Yes	85%
± 80 g	Yes	75%
± 90 g	Yes	65%
± 100 g	Yes	55%
± 110 g	Yes	45%
± 120 g	Yes	35%
± 130 g	Yes	25%
± 140 g	Yes	15%
± 150 g	Yes	5%
± 160 g	No	0%

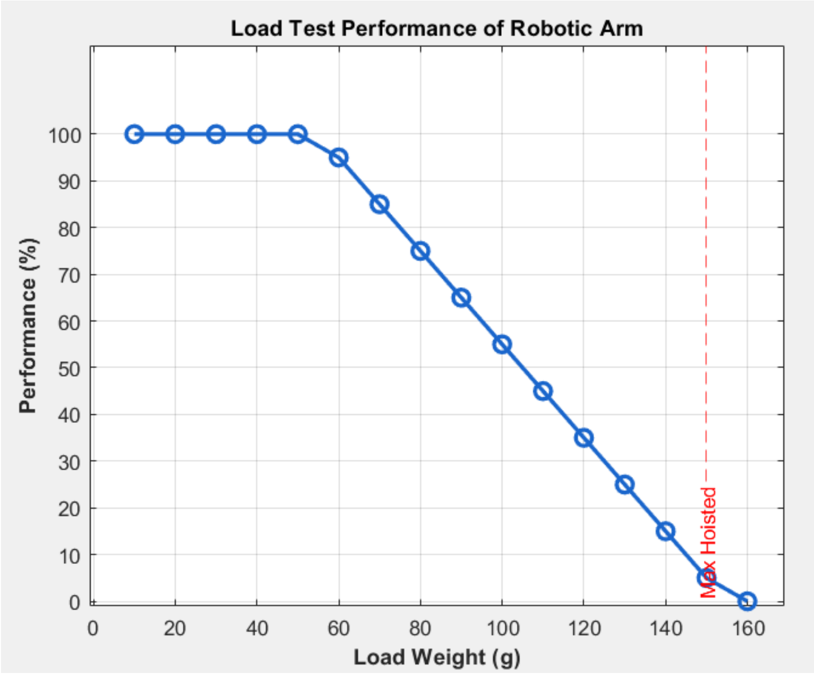

Figure 10. Load Test Plot

4. Conclusion

This study presents the design and development of a compact 3+1 DoF desktop robotic arm that integrates low-cost materials, additive manufacturing, and energy-efficient actuation systems. The proposed system demonstrates the feasibility of combining pulley-based transmission with stepper motor control to achieve a balance between mechanical performance, cost-effectiveness, and energy efficiency. The overall design approach emphasizes simplicity, modularity, and accessibility, making it suitable for educational purposes and small-scale automation applications. From an engineering perspective, the findings highlight the critical role of mechanical design integrity, transmission efficiency, and structural alignment in determining system performance. The study confirms that proper integration of lightweight structures with optimized transmission mechanisms can significantly enhance motion stability while minimizing energy consumption. These aspects are essential in advancing the development of sustainable robotic systems, where efficiency and resource utilization are key considerations.

In terms of sustainability, the use of additive manufacturing, reusable and industrially biodegradable materials contribute to reduced material waste and supports environmentally responsible production practices. The modular configuration further enhances the system's lifecycle by enabling easy maintenance, repair, and component replacement. Additionally, the implementation of low-power control systems aligns with the growing demand for energy-efficient automation technologies. Despite its contributions, the system remains limited by the absence of closed-loop feedback, constrained load capacity, and sensitivity to mechanical tolerances. These limitations indicate opportunities for future improvements, including the integration of sensor-based feedback control, enhancement of structural materials, and optimization of transmission systems. Further research may also explore the incorporation of intelligent control strategies and renewable energy integration to enhance both performance and sustainability. This study contributes to the advancement of affordable and sustainable robotic technologies by demonstrating that efficient, low-cost systems can be developed without compromising fundamental performance requirements. The proposed approach provides a practical foundation for future developments in educational robotics, lightweight automation systems, and sustainable engineering applications.

Acknowledgements

The Authors express sincere gratitude to the Center for Research and Community Service (CRCS), Sampoerna University, for providing the research grant and facilities.

CRediT Authorship Contribution Statement

Muhammad Shobri: Conceptualization, Methodology, Investigation, Data Curation, Writing Original Draft, Writing – Review & Editing, and Visualization; Ignatius Budi Sutanto Hadisujoto: Conceptualization, Methodology, Investigation, Data Curation, Formal Analysis and Supervision; Djati Wibowo: Methodology, Investigation, Data Curation, Formal Analysis and Supervision.

Conflicts of Interest

The authors declare that they have no known competing financial interests or personal relationships that could have appeared to influence the work reported in this paper.

Reference

[1] Zhang, XinLong, et al. "Validation Analysis of a Method for Determining the Ship's Vertical Centre of Gravity and Moment of Inertia Based on the Model Test." *Ships and Offshore Structures*, Aug. 2024, pp. 1–8, https://doi.org/10.1080/17445302.2024.2397274.

[2] Surati, Sharath, et al. *Pick and Place Robotic Arm: A Review Paper*. 2021, https://api.semanticscholar.org/CorpusID:236453923.

[3] Zamisyak, Oby, et al. *Educational Multifunction Robot (Indobot)Sebagai Robot Edukasi*. 2016, https://api.semanticscholar.org/CorpusID:114380274.

[4] Rerung, R.R., 2018. Technology adoption challenges among MSMEs in Indonesia. *International Journal of Business Innovation*, 3(2), pp.45–52.

[5] Partama, I.M., Dachyar, M., 2019. Analysis of industrial robot adoption in Indonesian SMEs. *IOP Conference Series: Materials Science and Engineering*, 598, 012045.

[6] Matúšová, M., Čarnogurský, J., Hroncová, D., 2019. Human factors and ergonomic risks in repetitive industrial tasks. *Applied Ergonomics*, 78, pp.1–8.

[7] Bakrewal, A., 2021. Cost-benefit analysis of robotic automation in manufacturing systems. *Procedia Computer Science*, 180, pp.521–530.

[8] Febrianto, E., 2024. Robotics in education: Enhancing engineering learning through hands-on systems. *Education and Information Technologies*, 29, pp.1123–1140.
[9] Adinandra, S., Nugroho, A., Wibowo, S., 2018. Development of low-cost robotic arms using open-source platforms. *International Journal of Mechanical Engineering and Technology*, 9(10), pp.125–134.
[10] García, E., Jiménez, M.A., De Santos, P.G., Armada, M., 2020. The evolution of robotics research: Transmission systems and actuation technologies. *Robotics and Autonomous Systems*, 124, 103388.
[11] Chowdhury, S., Yedavalli, R.K., 2016. Belt-driven robotic systems: Modeling and control. *IEEE/ASME Transactions on Mechatronics*, 21(2), pp.1033–1044.
[12] Qi, L., Wang, Y., Liu, H., 2024. Recent advances in lightweight robotic transmission systems. *Mechanism and Machine Theory*, 190, 105507.
[13] Siciliano, B., Khatib, O., 2019. *Springer Handbook of Robotics*, 2nd ed. Springer.
[14] Kröger, T., 2021. Industrial robotics: Programming, simulation and applications. *Annual Reviews in Control*, 52, pp.272–289.
[15] Villani, V., Pini, F., Leali, F., Secchi, C., 2018. Survey on human–robot collaboration in industrial settings. *Mechatronics*, 55, pp.248–266.
[16] Elfasakhany, A., Yanez, E., Baylon, K., Salgado, R., 2019. Design and development of a competitive low-cost robotic arm with four DOF. *Modern Mechanical Engineering*, 9(1), pp.1–12.
[17] Dhanabalan, T., Sathish, T., 2020. Transforming industrial automation through robotics and IoT. *Materials Today: Proceedings*, 37, pp.345–350.
[18] Kumar, R., Singh, R., Gehlot, A., 2021. Design and analysis of robotic arms using additive manufacturing. *Materials Today: Proceedings*, 44, pp.1320–1326.
[19] Ngo, T.D., Kashani, A., Imbalzano, G., Nguyen, K.T.Q., Hui, D., 2018. Additive manufacturing (3D printing): A review. *Composites Part B*, 143, pp.172–196.
[20] Attaran, M., 2017. The rise of 3D printing: The advantages of additive manufacturing. *Business Horizons*, 60(5), pp.677–688.
[21] Shneier, M., 2020. Robots in manufacturing: Recent trends and future outlook. *Robotics*, 9(4), 103.
[22] Li, Z., Wang, P., Liu, J., 2022. Low-cost robotic platforms for STEM education. *IEEE Access*, 10, pp.45678–45690.
[23] Hassan, M., Rahman, M., 2023. Energy-efficient robotic systems for sustainable manufacturing. *Journal of Cleaner Production*, 382, 135279.
[24] Kurniawan, A., Prasetyo, Y., 2022. Development of locally manufactured robotic systems for SMEs. *Sustainability*, 14(9), 5210.
[25] Wang, S., Chen, X., 2021. Design optimization of robotic arms using simulation tools. *Simulation Modelling Practice and Theory*, 109, 102278.
[26] Tay, C.C., Lim, H.N., Wong, K.Y., 2022. Design and development of SCARA robot for industrial automation. *International Journal of Advanced Manufacturing Technology*, 120, pp.1457–1472.
[27] Yamafuji, K., 2019. Fundamentals and applications of SCARA robots in precision assembly. *Robotics and Computer-Integrated Manufacturing*, 58, pp.1–10.

[28] Mashhadany, Y., Al-Samarraie, M., Abbas, H., 2024. High-speed SCARA robot control for precision applications. *IEEE Access*, 12, pp.34567–34578.
[29] Hirano, T., Fukuda, T., Arai, F., 2013. Cylindrical mobile robots for hazardous environments. *Advanced Robotics*, 27(5), pp.347–356.
[30] Patiny, L., 2021. Barycenter-based locomotion for cylindrical robots. *Robotics and Autonomous Systems*, 140, 103745.
[31] Franklin, J., Duran, C., Smith, R., 2020. Safety in collaborative robotics. *Safety Science*, 130, 104877.
[32] Chowdhury, S., Yedavalli, R.K., 2016. Dynamics of belt-driven systems. *Journal of Sound and Vibration*, 380, pp.1–16.
[33] Lee, J., Kim, D., Park, S., 2018. Planetary gear systems in robotics. *Mechanism and Machine Theory*, 122, pp.159–172.
[40] Fattah, A., 2021. Stepper motors in robotic applications. *International Journal of Electrical Engineering Education*, 58(4), pp.345–360.
[41] Kilburn, D., Daugherty, T., 1999. NEMA standards for stepper motors. *IEEE Industry Applications Magazine*, 5(3), pp.42–47.
[42] Zheng, Y., 2023. Servo motor control systems. *IEEE Transactions on Industrial Electronics*, 70(2), pp.1234–1243.
[43] Mthboob, M., Rahman, M., Karim, A., 2023. DC motor performance analysis. *Energy Reports*, 9, pp.1120–1132.
[44] Spong, M.W., Hutchinson, S., Vidyasagar, M., 2006. *Robot Modeling and Control*. Wiley.
[45] Craig, J.J., 2005. *Introduction to Robotics: Mechanics and Control*. Pearson.
[46] Beer, F.P., Johnston, E.R., 2015. *Vector Mechanics for Engineers*. McGraw-Hill.
[47] Khalil, W., Dombre, E., 2002. *Modeling, Identification and Control of Robots*. Butterworth-Heinemann.
[48] Transmission errors in belt drives, *Tribology International*, 2018.
[49] Mechanical misalignment in robotic systems, *Precision Engineering*, 2020.